Archives of Virology (2022) 167:2181–2191
https://doi.org/10.1007/s00705-022-05530-7

ORIGINAL ARTICLE

Immunogenic properties of SARS-CoV-2 inactivated by ultraviolet light

A. V. Gracheva[1] · E. R. Korchevaya[1] · Yu. I. Ammour[1] · D. I. Smirnova[1] · O. S. Sokolova[2] · G. S. Glukhov[2] · A. V. Moiseenko[2,3] · I. V. Zubarev[4] · R. V. Samoilikov[1] · I. A. Leneva[1] · O. A. Svitich[1,5] · V. V. Zverev[1,5] · Evgeny B. Faizuloev[1]

Received: 22 March 2022 / Accepted: 25 May 2022 / Published online: 20 July 2022

Abstract

Vaccination against COVID-19 is the most effective method of controlling the spread of SARS-CoV-2 and reducing mortality from this disease. The development of vaccines with high protective activity against a wide range of SARS-CoV-2 antigenic variants remains relevant. In this regard, evaluation of the effectiveness of physical methods of virus inactivation, such as ultraviolet irradiation (UV) of the virus stock, remains relevant. This study demonstrates that the UV treatment of SARS-CoV-2 completely inactivates its infectivity while preserving its morphology, antigenic properties, and ability to induce the production of virus-neutralizing antibodies in mice through immunization. Thus, the UV inactivation of SARS-CoV-2 makes it possible to obtain viral material similar in its antigenic and immunogenic properties to the native antigen, which can be used both for the development of diagnostic test systems and for the development of an inactivated vaccine against COVID-19.

Introduction

Vaccination against COVID-19 is the most effective method of controlling the spread of SARS-CoV-2 and reducing mortality from this disease. Vaccines based on viral vectors, self-replicating RNA, and recombinant and native viral antigens are widely used worldwide [1–5]. Despite unprecedented preventive measures and the widespread use of vaccines against COVID-19, the pandemic spread of the SARS-CoV-2 coronavirus continues even in countries with high vaccination coverage [6]. Several countries, including Russia, are affected by severe epidemiological conditions and high morbidity and mortality rates [6]. New strains of SARS-CoV-2, differing from the original Wuhan strain in their antigenic and biological properties, are reported regularly [7–9]. Thus, from August to November 2021, the genetic variant Delta B.1.617.2 of SARS-CoV-2, which replaced the Alpha, Beta, and Gamma variants, occupied at least 95% of the global incidence structure (https://www.gisaid.org/) [10]. The Delta variant has increased infectivity and is less efficiently neutralized by antisera obtained from recovered COVID-19 patients who had been infected with other variants [11–13]. Furthermore, the SARS-CoV-2 variant Omicron B.1.1.529 has high epidemiological significance and is classified by WHO as a variant of concern (VOC). The Omicron genome has several deletions and more than 30 amino acid substitutions in the S protein, resulting in increased binding affinity of the virus for the ACE-2 receptor and, consequently, increased transmissibility and ability to evade neutralizing antibodies [14]. Thus, research on the development of vaccines with high protective activity against a wide range of SARS-CoV-2 antigenic variants remains relevant.

According to WHO, 137 candidate COVID-19 vaccines are licensed or in clinical trials, while 194 candidates are in preclinical trials as of 14.01.2022 [15]. Among the 132

Handling Editor: Sheela Ramamoorthy.

✉ Evgeny B. Faizuloev
faizuloev@mail.ru

[1] I.I. Mechnikov Research Institute of Vaccines and Sera, Moscow 105064, Russia

[2] Faculty of Biology, Lomonosov Moscow State University, Moscow 119234, Russia

[3] N.N. Semenov Federal Research Center for Chemical Physics, Russian Academy of Sciences, Moscow 119991, Russia

[4] Faculty of Medicine, Lomonosov Moscow State University, Moscow 119991, Russia

[5] F.F. Erisman Institute of Public Health, I.M. Sechenov First Moscow State Medical University, Moscow 119991, Russia

vaccine candidates in various stages of clinical trials, 13% are inactivated-virus-based vaccines. The development of whole-virion inactivated vaccines is of particular interest, since such vaccines include the full set of structural viral proteins. The assurance of complete inactivation of the virus coupled with retaining the native conformation of the protective antigens is one of the most important requirements for whole-virion vaccines. Inactivated vaccines against COVID-19 are mainly produced by chemical methods based on the treatment of viral stock with β-propiolactone [5, 16–19] and/or formaldehyde [20]. Chemical inactivation can cause modifications and cross-linking of viral proteins, leading to conformational changes in viral antigens [21]. Furthermore, if toxic inactivating agents are used, additional steps are required to purify the viral antigen [16].

In this regard, evaluation of the effectiveness of physical methods of virus inactivation, such as ultraviolet irradiation of the virus stock, remains relevant. The aim of this work was to evaluate the effect of the SARS-CoV-2 virus inactivation with ultraviolet light (UV) on its morphology and antigenic and immunogenic properties. To achieve this goal, a preparation of UV-inactivated SARS-CoV-2 was obtained and investigated by immunochemical and virological methods.

Materials and methods

Virus and cells

Specimens of SARS-CoV-2 strains isolated in Vero cells in the Moscow region (Russia) belonging to different lineages, including the variants of concern Delta and Omicron, were used in the study (Table 1). Strain Dubrovka (GenBank ID: MW514307.1) [22], which is phylogenetically related to the Wuhan-Hu-1 strain (GenBank ID: NC_045512.2), was used for evaluation of immunogenic properties of UV-inactivated virus. All of the viruses (Table 1) were isolated and characterized by the authors of this study.

The virus was cultivated on the African green monkey kidney epithelial cell line Vero CCL81 (ATCC) (hereinafter referred to as Vero cells). Vero cells were maintained at 37°C in Earl-buffer-based DMEM medium (PanEco, Russia) in 5% fetal bovine serum (FBS) (Gibco, USA), with L-glutamine (PanEco) (300 μg/ml) and gentamicin (PanEco) (40 μg/ml) in an atmosphere of 5% CO_2. The neutralization reaction was performed using Earl-buffer-based DMEM nutrient medium supplemented with 1% FBS, L-glutamine (300 μg/ml), and gentamicin (40 μg/ml).

Mice

Female BALB/c mice, weighing 16-18 g (n = 25), obtained from the "Stezar" cattery (Russia), were used for immunization. The animals were kept in the animal facility of the I. I. Mechnikov Research Institute of Vaccines and Sera.

Sera from convalescent COVID-19 patients

Serum samples obtained from patients with a confirmed diagnosis of COVID-19 were provided by the Clinical Diagnostic Centre of the I. I. Mechnikov Research Institute of Vaccines and Sera. Work with clinical material was carried out under international ethical standards and with the consent of the patients.

Virus cultivation

A monolayer of Vero cells obtained within 72 hours of cultivation was infected with the Dubrovka strain of SARS-CoV-2 at different multiplicities of infection (MOI). Virus adsorption was carried out in a CO_2 incubator for 60 min, maintenance medium (DMEM, L-glutamine [300 μg/ml] and gentamicin [40 μg/ml]) was added, and the cells were incubated at 37°C in an atmosphere of 5% CO_2. To study the kinetics of virus reproduction, supernatants were collected every 12 hours for 4 days and stored at −80°C until tested by titration or quantitation by reverse-transcription real-time PCR.

Virus titration

SARS-CoV-2 titers were determined by the cytopathic effect endpoint method (CPE) in Vero cells. Four replicates of tenfold dilutions of the virus in maintenance medium were added to the wells of a 96-well plate and incubated for 5 days at 37°C in an atmosphere of 5% CO_2. The cell monolayer was inspected visually by microscopic examination for the

Table 1 Characteristics of SARS-CoV-2 specimens used in the study

Strain (isolate)	Collection date	GenBank ID of full genome sequence	Pangolin lineage	Variant of concern (WHO)	Passage level	Titer, log10 $TCID_{50}$/ml
Dubrovka	2020-06-04	MW514307.1	B.1.1.317	-	17	7.85
Altufjevo	2022-01-25	ON032859.1	B.1.1.529.1.1	Omicron	5	5.7
Podolsk	2021-10-08	ON032860.1	B.1.617.2.122	Delta	9	6.1

presence of characteristic CPE at 120 hours postinfection (rounding of cells and detachment of cells from the monolayer). The virus titer was calculated as described by Ramakrishnan et al. [23] and expressed as log10 $TCID_{50}$/ml.

MTT assay

The viability of virus-infected Vero cells was assessed by using the vital dye methyl thiazolyl tetrazolium (MTT) bromide. On day 5 postinfection, 20 µl of MTT solution (5 mg/ml; PanEco) was added to the cell-containing wells of the 96-well plate, which was incubated at 37°C in 5% CO_2 for 2 hours. Then, the medium was removed, and 100 µl of dimethyl sulfoxide (Sigma-Aldrich) was added to each well. Using a plate spectrophotometer, the OD of each well was measured at 530 nm, taking into account the baseline values at 620 nm. The viability of cells was calculated using the following formula:

$$\%\ Viability = \left(OD_{530}\ test\ sample / OD_{530}\ cell\ control\right) \times 100$$

where "OD_{530} test sample" is the mean OD_{530} value in the wells with infected cells and "OD_{530} cell control" is the mean OD_{530} value in the wells with uninfected cells.

Quantification of SARS-CoV-2 RNA

Viral RNA was isolated from culture samples using a MagnoPrime UNI reagent kit (NextBio, Russia) according to the manufacturer's instructions. To detect viral RNA, we used primers and a probe designed based on the sequence of the nucleocapsid N gene of SARS-CoV-2 virus – CoVN-F, COVN-R, and COVN-P, respectively (Table 2) – described by Chan et al. [24]. A 2.5x Taq-polymerase reaction mixture reagent kit and MMLV reverse transcriptase (Syntol, Russia) were used to perform reverse transcription (RT)-PCR. The reaction mixture contained 10 pmol of each primer, 5 pmol of the probe, Taq DNA polymerase, and 30 units of reverse transcriptase. The amplification program was as follows: one cycle of 45°C for 10 min, one cycle of 95°C for 5 min, and 45 cycles of 95°C for 5 s and 55°C for 45 s. The reaction was performed in a DTprime thermocycler (DNA-Technology, Russia). All primers and probes were synthesized at Syntol. Samples obtained by successive tenfold dilutions of a known concentration of the synthetic oligonucleotide COVN-PC (Table 2) were used to construct a calibration curve.

Inactivation of SARS-CoV-2 by ultraviolet (UV) light

The supernatant of infected Vero cells was collected 72 hours after infection with the virus, clarified by centrifugation at 4000 rpm, and titrated. Virus inactivation (titer, 8.75 log10 $TCID_{50}$/ml) was performed using a UV lamp (Philips TUV 30W/G30 T8, Holland). The length and diameter of the light tube were 895 mm and 28 mm, respectively, and the wavelength of the lamp was 253.7 nm. A Petri dish, 150 mm in diameter (177 cm^2), with 50 ml of viral material (5 mm thickness of the liquid layer), was placed under the lamp at a distance of 30 cm and irradiated for 0.5, 1, 2, 4, 6, 8, and 12 minutes with triple shaking of the liquid at equal time intervals (Fig. 1). Virus inactivation was monitored by three blind passages of the irradiated viral material on Vero cells, examining the cells for cytopathic effect and measuring the concentration of viral RNA in each of the passages.

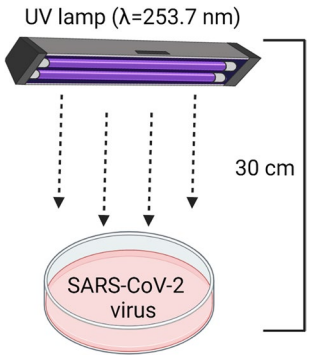

Fig. 1 The ultraviolet (UV) light irradiation system. A UV wavelength of 253.7 nm was used. The length and diameter of the light tube were 295 ± 3 mm and 15.5 ± 0.5 mm, respectively. SARS-CoV-2 with a titer of 8.75 log10 $TCID_{50}$/ml was placed in a 177-cm^2 dish, 30 cm below the UV-C light tube, and irradiated using for 0.5, 1, 2, 4, 6, 8, and 12 min at a UV-C intensity of 290 µW/cm^2. The image was made using the online program BioRender [https://biorender.com/about/]

Table 2 Primers, probes, and oligonucleotides used in this work

Name	Sequence (5′-3′)	Use	Source
CoVN-F	GCGTTCTTCGGAATGTCG	Forward primer	Chan et al. [24]
COVN-R	TTGGATCTCTTTGTCATCCAATTTG	Reverse primer	
COVN-P	FAM-AACGTGGTTGACCTACAGGT-BHQ1	Probe	
COVN-PC	GCGTTCTTCGGAATGTCGCGCGCATTGGCATGGAAGTCACCTTCG GAACCTTCGGAACGGAACGTGTGTTGACACCTACAGGTGCCATCA AATTGGAATGACAAAGATCCAA	Calibration	This work

The intensity of UV-C radiation was measured using a UV radiometer with a TKA-PKM (13) attenuating filter (NTP TKA LLC, Russia). For use in the ELISA and immunochromatography (IC) tests, 45 ml of UV-inactivated virus-containing supernatant (8.75 log10 $TCID_{50}$/ml) was clarified by centrifugation and passed through a 100-kDa Amicon MWCO centrifuge filter (Millipore, Ireland) at 4000 rpm. The virus preparation collected on the filter was diluted to 4.5 ml with sterile PBS (pH 7.2), achieving a tenfold concentration of SARS-CoV-2 virions. Before use, the preparation was processed on an MSE ultrasonic disintegrator (UK) at an amplitude of 2 for 2 minutes.

Evaluation of the antigenic properties of UV-inactivated SARS-CoV-2

Fivefold dilutions of UV-inactivated SARS-CoV-2 were analyzed by ELISA and immunochromatography (IC), determining the highest dilution that gave a positive result. The SARS-CoV-2 antigen was detected in the IC reaction using a SARS-CoV-2 Rapid Antigen Test reagent kit (SD Biosensor Inc, Republic of Korea) according to the instructions. To determine the detection limit of SARS-CoV-2 antigen by ELISA, fivefold dilutions of UV-inactivated SARS-CoV-2 concentrated on 100-kDa Amicon MWCO columns (Millipore, Ireland) were coated onto into 96-well immunoassay plates (Costar 2592 High-binding). ELISA was performed using sera from convalescent COVID-19 patients at dilution 1:200, using a BioKit ELISA reagent kit (Bioservis, Russia) according to the instructions. Horseradish-peroxidase-labeled murine monoclonal antibodies to the Fc fragment of human γ-globulin (Bioservis, Russia) at a dilution of 1:60,000 were used for detection.

Immunization of mice

To assess the immunogenicity of the inactivated virus, female BALB/c mice (n = 25) were divided into five groups of five animals and injected subcutaneously into the withers with 200 µL of the virus preparation twice with a 21-day interval according to the protocol shown in Table 3.

Virus-UV, UV-inactivated SARS-CoV-2 virus; CFA, complete Freund's adjuvant; IFA, incomplete Freund's adjuvant; PBS, phosphate-buffered saline, pH 7.4

Viral material was mixed with adjuvants so that each mouse received a dose corresponding to 7.0 log10 $TCID_{50}$. Mice in the control group were injected with PBS. On the day of the first immunization and 2 weeks after each immunization, blood samples were collected from the tail vein of the animals.

Immediately before immunization, viral material was mixed with an equal volume of Freund's adjuvant (CFA or IFA) (Difco Laboratories, USA) and repeatedly (at least 15 times) passed through a fine injection needle. The emulsion was administered to the experimental animals within 10 min after preparation.

The viral material was adsorbed onto aluminum hydroxide (Sigma) so that a single injection dose (200 µL) contained 1.7 µg of adjuvant. The resulting mixture was incubated with regular shaking for 24 hours at +4°C before use.

Antibody titration of mouse sera by ELISA

Determination of antibody titers against SARS-CoV-2 in mouse sera was performed using a BioKit ELISA reagent kit (Bioservis, Russia) according to the instructions. Native viral antigen obtained as described above was coated at a dilution of 1:100 onto the wells of an immunoassay plate. Duplicate dilutions of the sera were analyzed by ELISA, starting at a dilution of 1:50. Horseradish-peroxidase-conjugated goat anti-mouse IgG, IgA, and IgM antibodies (IMTEC, Russia) were used in a dilution of 1:10,000 for detection of murine antibodies. The reciprocal value of the last dilution at which the OD value of the sample was higher than the cutoff for each assay was taken as the titer of SARS-CoV-2 antibodies. The OD value for the negative serum multiplied by 2 was used as the cutoff.

Neutralization reaction

Titers of SARS-CoV-2-neutralizing antibodies (NA) were determined as described by Gracheva et al. [22]. Frozen serum samples (100 µL) were thawed and heated at 56°C for 30 min, and twofold serial dilutions were prepared using maintenance medium. The serum dilutions were then mixed with an equal volume of a SARS-CoV-2 preparation containing 2×10^3 $TCID_{50}$/ml and incubated at 37°C in a 5% CO_2 atmosphere for 1 h. A 100-µL aliquot of the mixture of virus and serum was then added to a three-day monolayer

Table 3 Protocol for immunization of mice with UV-inactivated SARS-CoV-2

Group of mice	1 (n = 5)	2 (n = 5)	3 (n = 5)	4 (n = 5)	5 (n = 5)
First immunization	Virus-UV	Virus-UV +CFA	Virus-UV + $Al(OH)_3$	Infectious SARS-CoV-2	PBS
Second immunization (21 days later)	Virus-UV	Virus-UV +IFA	Virus-UV + $Al(OH)_3$	-	PBS

of Vero cells in a 96-well plate in four replicates (viral dose, 100 $TCID_{50}$ per well) and incubated for 5 days at 37 °C in a 5% CO_2 atmosphere. In addition to the test samples, the following controls were included: cell control (uninfected cell culture), virus control (cells infected with a working dilution of virus), serum control (serum diluted 1:20), and dose control (fivefold dilutions of virus). The neutralization reaction result was recorded visually by microscopic examination of the cell monolayer on day 5. The neutralizing titer was defined as the reciprocal value of the last dilution at which no signs of CPE were detected in two or more wells.

Transmission electron microscopy

The samples were applied to glow-discharged TEM grids with carbon support film (TedPella Carbon Type B, 300 mesh). The grids were then negatively stained with 1% uranium acetate. TEM images were acquired using a JEOL JEM-2100 200-kV electron microscope (Japan) equipped with Gatan Orius SC200D camera (2k x 2k) (USA). Negatively stained samples were imaged at magnification yielding a 3.4-Å pixel size with −1.5 µm defocus applied.

Statistical processing of the data

Statistical data processing was performed using GraphPad Prism v.5.03 software. The correlation of virus titer and viral RNA concentration was evaluated using Spearman's test at a 95% confidence interval. The significance of the difference was determined using Student's *t*-test at a 95% confidence interval.

Work safety requirements

All work with SARS-CoV-2 was carried out under biosafety level 3 conditions.

Results

Virus accumulation and ultraviolet (UV) inactivation

The growth kinetics of SARS-CoV-2 strain Dubrovka, and viral RNA replication in Vero cells at different multiplicities of infection (MOI), 0.001 and 0.00001, were studied to determine the conditions for producing viral material with high titer. Plots of the accumulation of infectious virus and viral RNA in cells are shown in Figure 2.

With an MOI of 0.001, the virus titer reached maximum values by 36 hours postinfection (p.i.) and remained at 8.25-8.75 log10 $TCID_{50}$/ml at 36-72 hours p.i., after which it decreased and reached 4.75 log10 $TCID_{50}$/ml at 96 hours p.i. At an MOI of 0.00001, the virus titer reached a maximum of 9.0 log10 $TCID_{50}$/ml at 48 hours p.i. It remained at this level until 84 hours p.i. and decreased to 6.5 log10 $TCID_{50}$/ml at 96 hours p.i.

The pattern of viral RNA accumulation was generally consistent with the viral titer curve, except for the period after 84 hours p.i., when the viral titers started to decrease, whereas the RNA content remained at a maximum of approximately 11.0 log10 RNA copies/ml until 96 hours p.i. The data obtained by titration correlated significantly with the results obtained by real-time RT-PCR between 12 and 84 hours p.i. (MOI 0.001, Spearman $\rho = 1.000$, $P < 0.05$, MOI 0.00001 Spearman $\rho = 1.000$, $P < 0.05$).

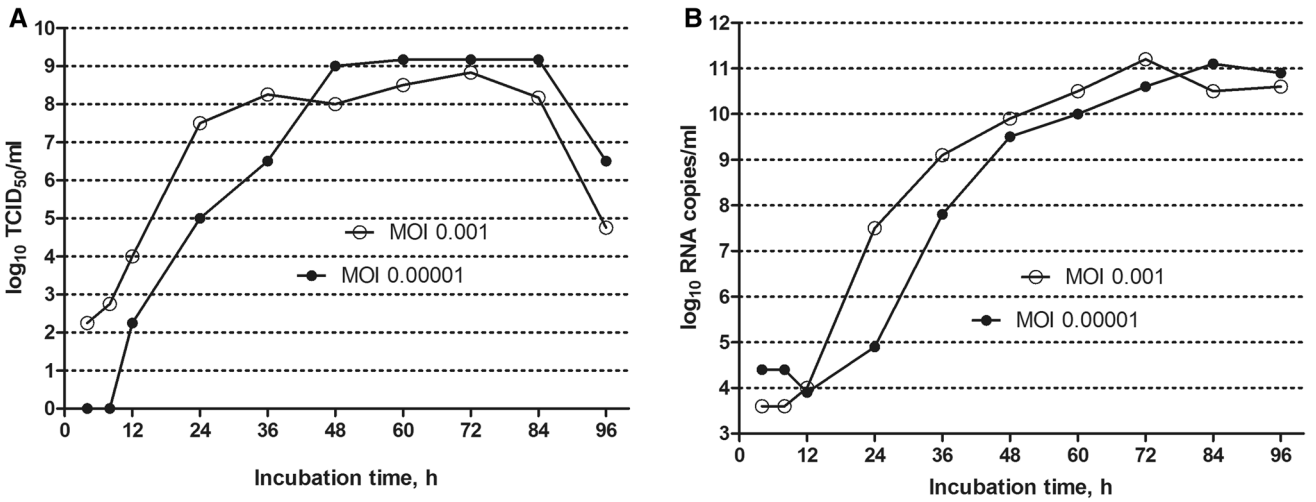

Fig. 2 Growth kinetics of SARS-CoV-2 (Dubrovka strain) in Vero cells. (**A**) Virus titer. (**B**) Viral RNA concentration. Cells were inoculated at an MOI of 0.001 and 0.00001. Supernatant samples were collected every 12 hours to titrate the virus and determine the concentration of viral RNA

Table 4 Effectiveness of SARS-CoV-2 (Dubrovka strain) inactivation by UV light with different irradiation regimes at a UV-C intensity of 290 μW/cm^2

Exposure time, min	0.0	0.5	1	2	4	8	12
Virus titer (log10 $TCID_{50}$/ml)	8.75 ± 0.27	6.75 ± 0.18	4.0 ± 0.40	2.0 ± 0.21	n/d	n/d	n/d
Residual infectivity (%)	100	1.0	1.8×10^{-2}	1.8×10^{-5}	0.0	0.0	0.0
Degree of inactivation (%)	0.0	99.00	99.98	>99.99	100	100	100

n/d - not detected

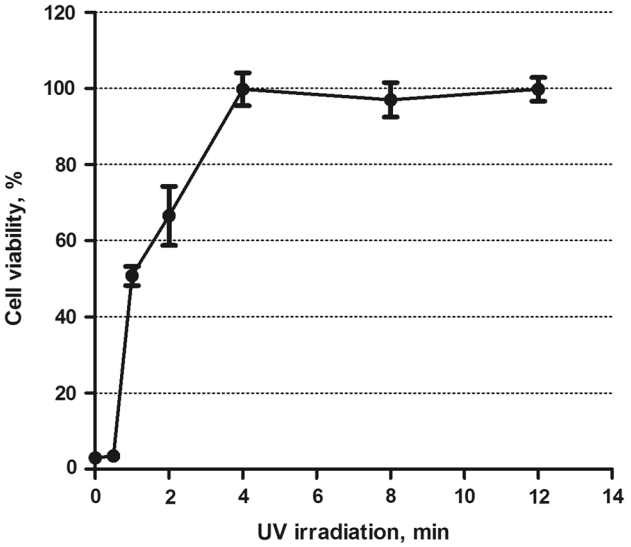

Fig. 3 Survival of Vero cells on day 5 after inoculation with a UV-inactivated SARS-CoV-2 preparation. The virus preparation was irradiated for the indicated times at a UV-C intensity of 290 μW/cm^2. Inactivation of the virus was confirmed by blind passage in Vero cells. Vero cell survival was measured using an MTT test

For viral antigen production, Vero cells were infected with SARS-CoV-2 at an MOI of 0.00001, and the virus-containing supernatants were collected at 72 hours p.i., yielding viral material with a titer of 8.75 log10 $TCID_{50}$/ml and a viral RNA concentration of 9.5 log10 copies/ml. The viral material was treated with UV light for different lengths of time, from 30 s to 12 min, and the degree of virus inactivation was assessed (Table 4).

Complete inactivation of the virus was observed upon irradiation for 4 minutes or more, which was confirmed in five independent experiments in which residual infectivity was tested by three blind passages in Vero cell culture. The survival rate of Vero cells inoculated with irradiated virus preparations increased with increasing irradiation time (Fig. 3).

It was found that UV exposure for 4, 8, and 12 minutes resulted in complete inactivation of the Altufjevo and Podolsk isolates of SARS-CoV-2, which belongs to Omicron and Delta variants of concern. In further work, viral material treated with UV light for 4 min was used to evaluate the antigenic and immunogenic properties of the virus.

Structural characterization of UV-inactivated SARS-CoV-2

In the UV-inactivated SARS-CoV-2 (Dubrovka strain) preparation, TEM revealed virus-like particles with morphodiagnostic features of a coronavirus. The virions had a round shape with characteristic 12- to 15-nm spikes on the shell, and the virion diameter was 90-110 nm (Fig. 4). The shape and size of these virus-like particles are in good agreement with the previously obtained microphotographs of β-propiolactone-inactivated particles of SARS-CoV-2 [5].

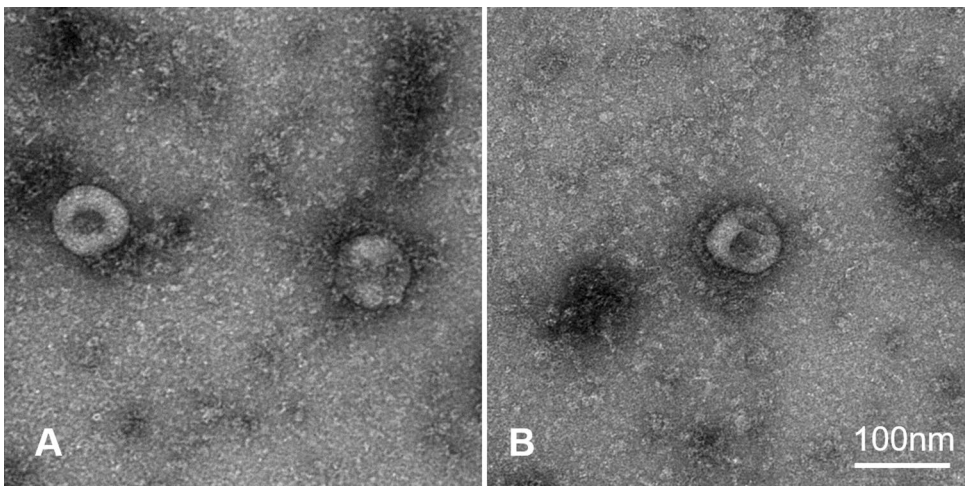

Fig. 4 Electron micrograph of negatively stained UV-inactivated SARS-CoV-2 at 40 000× magnification. The arrow shows characteristic spikes (S-protein) on the surface of the coronavirus. Panels **A** and **B** represent different fields of view for the same preparation of the Dubrovka strain

Antigenic properties and immunogenicity of UV-inactivated SARS-CoV-2

The antigenic properties of the virus after UV treatment were assessed using a rapid immunochromatographic (IC) test for the presence of the SARS-CoV-2 antigen and by ELISA. In the UV-inactivated SARS-CoV-2 (Dubrovka strain) preparation, the viral antigen was detected up to a dilution of 1:15,625 by IC, whereas by ELISA it was detected up to a dilution of 1:78,125 (Fig. 5, Table 5).

The Dubrovka strain was chosen for the study of immunogenicity of UV-inactivated SARS-CoV-2, since it had the highest growth rate and titer (Table 1). It was observed that mice immunized with Freund's adjuvant had lost significant weight. On day 8 after the second immunization, the difference in weight compared to the control group was 12% ($p < 0.05$), while the mice in the other groups did not differ in weight from those in the control group.

After the first immunization, the blood of animals immunized with UV-inactivated SARS-CoV-2 with Freund's adjuvant and aluminum hydroxide showed detectable amounts of antibodies to SARS-CoV-2 by ELISA. After the second immunization, antibodies to the virus were detected in the blood of immunized animals of all groups, with the highest titers of antibodies achieved when Freund's adjuvant (13120 ± 8497) or aluminum hydroxide (1320 ± 1163) was included in the preparation (Fig. 6A).

The main criterion for evaluating immunogenic properties was the ability of UV-inactivated SARS-CoV-2 to induce neutralizing antibody (NAb) production in animals. After the first immunization, NAbs were detected in the blood of animals immunized with UV-inactivated SARS-CoV-2. After the second immunization, NAb titers increased by an average of 20- to 40-fold. NAb titers were significantly higher in mice immunized with a preparation containing Freund's adjuvant (448 ± 520) than in mice immunized with preparations containing aluminum hydroxide (96 ± 128) or without adjuvant (62 ± 261), $p < 0.01$ (Fig. 6B).

In the group of mice injected with live virus, 2 weeks after immunization, antibodies to SARS-CoV-2 were detected in both ELISA (2760 ± 561) and the neutralization assay (308 ± 544), and at a higher titer than when the

Fig. 5 Detection of viral antigen in a UV-inactivated SARS-CoV-2 preparation by immunochromatography (IC). A SARS-CoV-2 Rapid Antigen Test kit was used to test sequential fivefold dilutions of UV-inactivated SARS-CoV-2 from 1:5 to 1:15,625 (1-6), a positive control (K+), and a negative control (K-)

Table 5 Results of detection of viral antigen in UV-inactivated SARS-CoV-2 by ELISA and IC

Dilution	1:5	1:25	1:125	1:625	1:3125	1:15625	1:78125	1:390625
IC	+	+	+	+	+	+	-	-
ELISA* (OD ± SD)	**3.27 ± 0.13**	**3.16 ± 0.09**	**2.38 ± 0.52**	**1.62 ± 0.81**	**1.07 ± 0.49**	**0.43 ± 0.18**	**0.20 ± 0.07**	0.10 ± 0.04

*ELISA results for sera from five convalescent COVID-19 patients. The UV-inactivated SARS-CoV-2 antigen was coated onto an immunological plate and analyzed by ELISA with patients' sera at a dilution of 1:200. The cutoff value of the ELISA was 0.15

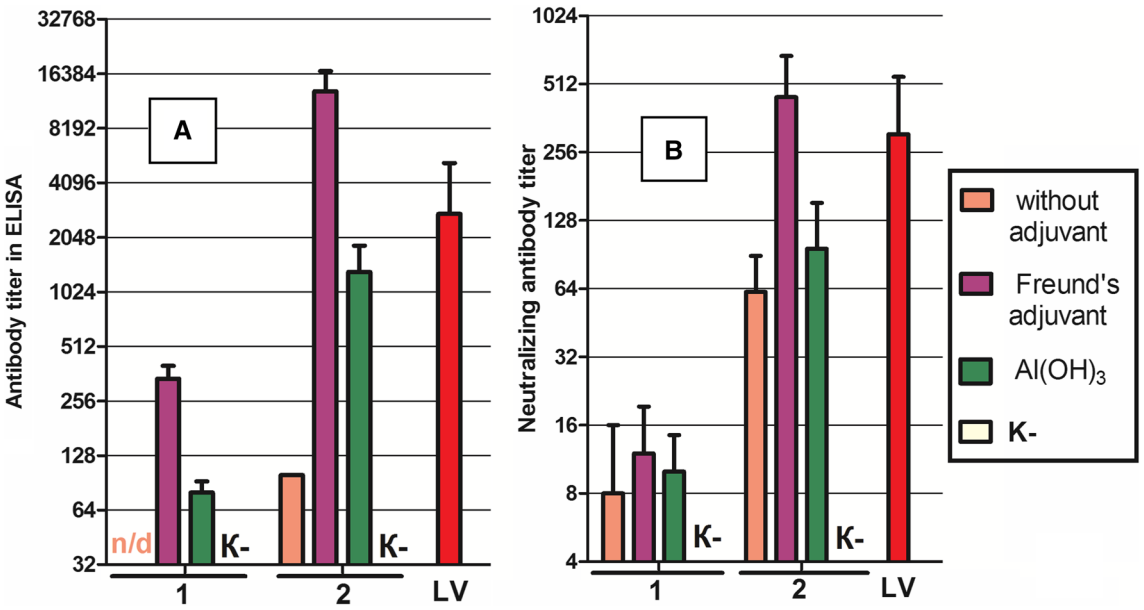

Fig. 6 Mean antibody titers to SARS-CoV-2 in the sera of mice after the first and second immunization. (**A**) Antibody titer in ELISA. (**B**) Neutralizing antibody titer. 1, 14 days after the first immunization with UV-inactivated virus; 2, 14 days after the second immunization with UV-inactivated virus; LV, 14 days after immunization with live SARS-CoV-2; K, mice injected with PBS

corresponding dose of UV-inactivated SARS-CoV-2 with different adjuvants was injected ($p < 0.01$) (Fig. 6).

In the control group (K-) animals, no antibodies to the virus were detected by ELISA or in the neutralization assay (Fig. 6).

Discussion

Inactivated virus preparations have traditionally been used in the production of vaccines [24]. Inactivated vaccines are safe and effective for preventing influenza, polio, hepatitis A, tick-borne encephalitis, Japanese encephalitis [25–29], and COVID-19 [5, 16–20]. In most cases, inactivated vaccine production technology involves chemical inactivation of the virus. However, there are examples of the use of ultraviolet radiation for the production of promising vaccine preparations against SARS-CoV, herpes simplex virus, porcine epidemic diarrhea coronavirus, measles virus, rabies virus, influenza virus, and monkey immunodeficiency virus [30–36]. A high efficiency of a UV-inactivated preparation of rabies virus for emergency prevention of rabies has been reported [34]. A UV-inactivated preparation of SARS-CoV in the work of Iwata-Yoshikawa et al. [37] protected immunized mice against challenge with a wild strain of the virus. Ultraviolet light disinfection has been used successfully in medical facilities and laboratories dealing with SARS-CoV-2 [38] and other pathogens. However, the use of UV inactivation of SARS-CoV-2 for vaccine production has not been described in the scientific literature.

Ultraviolet radiation is divided into three wavelength ranges: UV-A (320-400 nm), UV-B (280-320 nm), and UV-C (200-280 nm). UV-C is the most powerful ultraviolet radiation of the three, and is used for disinfection [38–40]. Therefore, in our work, we treated viral material with UV-C at 253.7 nm. UV radiation causes photochemical damage to viral nucleic acids by inducing dimerization of adjacent pyrimidine nucleotides, which disrupts the transcription and replication of the viral genome [40]. Since RNA-containing viruses usually have ineffective mechanisms of genome repair, they can be easily inactivated by UV radiation [38–40]. It is important to mention that ultraviolet light effectively inactivates viruses while preserving the integrity of epitopes, which allows the use of preparations of UV-inactivated viruses in the production of diagnostic test systems and vaccines [33, 34, 37, 39, 40]. Since UV irradiation causes non-specific damage to viral RNA, we believe that the results obtained on three antigenically different strains of SARS-CoV-2 (Dubrovka, Altufjevo, and Podolsk) are applicable to other SARS-CoV-2 strains.

Widely used chemical methods of virus inactivation involve the use of highly toxic substances such as β-propiolactone, classified as a potent carcinogen to humans (group 2B carcinogen), and formaldehyde, classified as carcinogenic to humans (group 1 carcinogen) by the International Agency for Research on Cancer [41]. For this reason, physical methods of virus inactivation such as UV

irradiation are preferred in vaccine production technology, as they do not involve the treatment of the virus with harmful substances and therefore do not require the introduction of additional steps to purify the viral antigen from toxic compounds.

In this study, ELISA and IC methods revealed the ability of UV-inactivated SARS-CoV-2 to bind to antibodies in convalescent sera at high dilutions of viral antigen up to 1:78,125 (Table 4), indicating that the antigenic determinants were preserved. When injected subcutaneously into mice, UV-inactivated SARS-CoV-2, both in its free form and complexed with adjuvants, induced the production of antibodies to structural proteins of the virus, including antibodies directed to neutralizing epitopes of the S protein. The ability of UV-inactivated SARS-CoV-2 to induce the production of neutralizing antibodies as the main indicator of specific protective activity for whole-virion-inactivated vaccines was highlighted in this work. Furthermore, SARS-CoV-2, inactivated at the minimum dose required for inactivation by UV irradiation, was used for immunization to minimize damage to the antigenic determinants of viral antigens. TEM revealed coronavirus virions with highly conserved spikes consisting of the S protein in the UV-inactivated SARS-CoV-2 preparation, which is consistent with the observed immunogenicity of the preparation.

The results showed that the immunogenicity of UV-inactivated SARS-CoV-2 can be enhanced by the use of adjuvants, with Freund's adjuvant being the most effective. However, the immunogenicity of live SARS-CoV-2 in mice was higher than that of UV-inactivated SARS-CoV-2 variants, even when injected in the presence of adjuvants (Fig. 6). Although SARS-CoV-2 is not pathogenic to mice, it readily adapts to reproduce in mouse lungs and is capable of inducing a distinct humoral immune response in animals [42–45]. Therefore, it seems reasonable that the infection of mice with an infectious virus induces a stronger humoral immune response than the administration of a corresponding dose of UV-inactivated SARS-CoV-2.

Conclusion

Treatment of SARS-CoV-2 with UV light completely inactivates its infectivity while preserving its morphology, antigenic properties, and ability to induce the production of virus-neutralizing antibodies in mice after immunization. Thus, the inactivation of SARS-CoV-2 by UV makes it possible to obtain viral material similar in its antigenic and immunogenic properties to the native antigen, which can be used both for diagnostic purposes (ELISA, immunoblotting, IC assay) and for the development of an inactivated vaccine against COVID-19.

Acknowledgements The study was carried out using equipment of the Collective Usage Center "I. I. Mechnikov NIIVS", Moscow, Russia. Electron microscopy was performed using the unique equipment setup "3D-EMS" of Moscow State University.

Author contributions All authors contributed to the study's conception and design. Material preparation, data collection, and analysis were performed by Gracheva A.V., Faizuloev E.B., Korchevaya E.R., Smirnova D.I., and Samoilikov, R.V. Electron microscopy was performed by Sokolova O.S, Glukhov G.S, Moiseenko A.V. and Zubarev I.V. The first draft of the manuscript was written by Gracheva A.V., Faizuloev E.B., and Ammour Yu. I., and all authors commented on previous versions of the manuscript. All authors read and approved the final manuscript.

Funding The research was supported by the Russian Foundation for Basic Research under research project no. 20-04-60079. Electron microscopy was performed with the support of the Russian Foundation for Basic Research under research project no. 20-04-60258.

Declarations

Conflict of interest The authors declare that they have no conflict of interest.

Ethical approval All applicable international, national, and/or institutional guidelines for the care and use of animals, including the Guide for the Care and Use of Laboratory Animals [46], were followed. This study was approved by the Medical Ethics Review Committee of the I. I. Mechnikov Research Institute of Vaccines and Sera (Ethics Committee Decision No 2 dated May 24, 2021).

References

1. Francis AI, Ghany S, Gilkes T et al (2021) Review of COVID-19 vaccine subtypes, efficacy and geographical distributions. Postgrad Med J. https://doi.org/10.1136/postgradmedj-2021-140654
2. Marfe G, Perna S, Shukla AK (2021) Effectiveness of COVID-19 vaccines and their challenges (Review). Exp Ther Med. https://doi.org/10.3892/etm.2021.10843
3. Picazo JJ (2021) Vacuna frente al COVID-19 [Vaccine against COVID-19]. Rev Esp Quimioter. Spanish. https://doi.org/10.37201/req/085.2021.
4. Kandimalla R, Chakraborty P, Vallamkondu J, Chaudhary A, Samanta S, Reddy PH, De Feo V, Dewanjee S (2021) Counting on COVID-19 vaccine: insights into the current strategies, progress and future challenges. Biomedicines. https://doi.org/10.3390/biomedicines9111740
5. Kozlovskaya LI, Piniaeva AN, Ignatyev GM, Gordeychuk IV, Volok VP, Rogova YV, Shishova AA, Kovpak AA, Ivin YY, Antonova LP, Mefyod KM, Prokosheva LS, Sibirkina AS, Tarasova YY, Bayurova EO, Gancharova OS, Illarionova VV, Glukhov GS, Sokolova OS, Shaitan KV, Moysenovich AM, Gulyaev SA, Gulyaeva TV, Moroz AV, Gmyl LV, Ipatova EG, Kirpichnikov MP, Egorov AM, Siniugina AA, Ishmukhametov AA (2021) Long-term humoral immunogenicity, safety and protective efficacy of inactivated vaccine against COVID-19 (CoviVac) in preclinical studies. Emerg Microbes Infect. https://doi.org/10.1080/22221751.2021.1971569
6. WHO Coronavirus (COVID-19) Dashboard | WHO Coronavirus (COVID-19) dashboard with vaccination data. https://covid19.who.int/. Accessed 23 Feb 2022

7. Gómez-Carballa A, Pardo-Seco J, Bello X, Martinón-Torres F, Salas A (2021) Superspreading in the emergence of COVID-19 variants. Trends Genet. https://doi.org/10.1016/j.tig.2021.09.003
8. Nikonova AA, Faizuloev EB, Gracheva AV, Isakov IY, Zverev VV (2021) Genetic diversity and evolution of the biological features of the pandemic SARS-CoV-2. Acta Nat. https://doi.org/10.32607/actanaturae.11337
9. Choi JY, Smith DM (2021) SARS-CoV-2 variants of concern. Yonsei Med J. https://doi.org/10.3349/ymj.2021.62.11.961
10. Mathieu E, Ritchie H, Ortiz-Ospina E et al (2021) A global database of COVID-19 vaccinations. Nat Hum Behav 5:947–953. https://doi.org/10.1038/s41562-021-01122-8
11. Dupont L, Snell LB, Graham C, Seow J, Merrick B, Lechmere T, Maguire TJA, Hallett SR, Pickering S, Charalampous T, Alcolea-Medina A, Huettner I, Jimenez-Guardeño JM, Acors S, Almeida N, Cox D, Dickenson RE, Galao RP, Kouphou N, Lista MJ, Ortega-Prieto AM, Wilson H, Winstone H, Fairhead C, Su JZ, Nebbia G, Batra R, Neil S, Shankar-Hari M, Edgeworth JD, Malim MH, Doores KJ (2021) Neutralizing antibody activity in convalescent sera from infection in humans with SARS-CoV-2 and variants of concern. Nat Microbiol. https://doi.org/10.1038/s41564-021-00974-0
12. Tao K, Tzou PL, Nouhin J, Gupta RK, de Oliveira T, Kosakovsky Pond SL, Fera D, Shafer RW (2021) The biological and clinical significance of emerging SARS-CoV-2 variants. Nat Rev Genet. https://doi.org/10.1038/s41576-021-00408-x
13. Saito A et al (2021) Enhanced fusogenicity and pathogenicity of SARS-CoV-2 Delta P681R mutation. Nature. https://doi.org/10.1038/s41586-021-04266-9
14. Lu L, Mok BW, Chen LL, Chan JM, Tsang OT, Lam BH, Chuang VW, Chu AW, Chan WM, Ip JD, Chan BP, Zhang R, Yip CC, Cheng VC, Chan KH, Jin DY, Hung IF, Yuen KY, Chen H, To KK (2021) Neutralization of SARS-CoV-2 Omicron variant by sera from BNT162b2 or Coronavac vaccine recipients. Clin Infect Dis. https://doi.org/10.1093/cid/ciab1041
15. COVID-19 vaccine tracker and landscape. https://www.who.int/publications/m/item/draft-landscape-of-covid-19-candidate-vaccines. Accessed 23 Feb 2022
16. Gao Q, Bao L, Mao H, Wang L, Xu K, Yang M, Li Y, Zhu L, Wang N, Lv Z, Gao H, Ge X, Kan B, Hu Y, Liu J, Cai F, Jiang D, Yin Y, Qin C, Li J, Gong X, Lou X, Shi W, Wu D, Zhang H, Zhu L, Deng W, Li Y, Lu J, Li C, Wang X, Yin W, Zhang Y, Qin C (2020) Development of an inactivated vaccine candidate for SARS-CoV-2. Science. https://doi.org/10.1126/science.abc1932
17. Wu Z, Hu Y, Xu M, Chen Z, Yang W, Jiang Z, Li M, Jin H, Cui G, Chen P, Wang L, Zhao G, Ding Y, Zhao Y, Yin W (2021) Safety, tolerability, and immunogenicity of an inactivated SARS-CoV-2 vaccine (CoronaVac) in healthy adults aged 60 years and older: a randomised, double-blind, placebo-controlled, phase 1/2 clinical trial. Lancet Infect Dis. https://doi.org/10.1016/S1473-3099(20)30987-7
18. Wang H, Zhang Y, Huang B, Deng W, Quan Y, Wang W, Xu W, Zhao Y, Li N, Zhang J, Liang H, Bao L, Xu Y, Ding L, Zhou W, Gao H, Liu J, Niu P, Zhao L, Zhen W, Fu H, Yu S, Zhang Z, Xu G, Li C, Lou Z, Xu M, Qin C, Wu G, Gao GF, Tan W, Yang X (2020) Development of an inactivated vaccine candidate, BBIBP-CorV, with potent protection against SARS-CoV-2. Cell. https://doi.org/10.1016/j.cell.2020.06.008
19. Ella R, Reddy S, Blackwelder W, Potdar V, Yadav P, Sarangi V, Aileni VK, Kanungo S, Rai S, Reddy P, Verma S, Singh C, Redkar S, Mohapatra S, Pandey A, Ranganadin P, Gumashta R, Multani M, Mohammad S, Bhatt P, Kumari L, Sapkal G, Gupta N, Abraham P, Panda S, Prasad S, Bhargava B, Ella K, Vadrevu KM, COVAXIN Study Group (2021) Efficacy, safety, and lot-to-lot immunogenicity of an inactivated SARS-CoV-2 vaccine (BBV152): interim results of a randomised, double-blind, controlled, phase 3 trial. Lancet. https://doi.org/10.1016/S0140-6736(21)02000-6
20. Zakarya K, Kutumbetov L, Orynbayev M, Abduraimov Y, Sultankulova K, Kassenov M, Sarsenbayeva G, Kulmagambetov I, Davlyatshin T, Sergeeva M, Stukova M, Khairullin B (2021) Safety and immunogenicity of a QazCovid-in® inactivated whole-virion vaccine against COVID-19 in healthy adults: a single-centre, randomised, single-blind, placebo-controlled phase 1 and an open-label phase 2 clinical trials with a 6 months follow-up in Kazakhstan. EClinicalMedicine. https://doi.org/10.1016/j.eclinm.2021.101078
21. Liu C, Mendonça L, Yang Y, Gao Y, Shen C, Liu J, Ni T, Ju B, Liu C, Tang X, Wei J, Ma X, Zhu Y, Liu W, Xu S, Liu Y, Yuan J, Wu J, Liu Z, Zhang Z, Liu L, Wang P, Zhang P (2020) The architecture of inactivated SARS-CoV-2 with postfusion spikes revealed by Cryo-EM and Cryo-ET. Structure. https://doi.org/10.1016/j.str.2020.10.001
22. Gracheva AV, Korchevaya ER, Kudryashova AM, Borisova OV, Petrusha OA, Smirnova DI, Chernyshova IN, Svitich OA, Zverev VV, Faizuloev EB (2021) Adaptation of the MTT assay for detection of neutralizing antibodies against the SARS-CoV-2 virus. J Microbiol Epidemiol Immunobiol. https://doi.org/10.36233/0372-9311-136
23. Ramakrishnan MA (2016) Determination of 50% endpoint titer using a simple formula. World J Virol. https://doi.org/10.5501/wjv.v5.i2.85
24. Chan JF, Yip CC, To KK, Tang TH, Wong SC, Leung KH et al (2020) Improved molecular diagnosis of COVID-19 by the novel, highly sensitive and specific COVID-19-RdRp/Hel real-time reverse transcription-PCR assay validated in vitro and with clinical specimens. J Clin Microbiol. https://doi.org/10.1128/JCM.00310-20
25. Yuan Y, Wang RT, Xia J, Cao HJ (2021) Interventions for preventing influenza: an overview of Cochrane systematic reviews and a Bayesian network meta-analysis. J Integr Med. https://doi.org/10.1016/j.joim.2021.09.001
26. Stuurman AL, Marano C, Bunge EM, De Moerlooze L, Shouval D (2017) Impact of universal mass vaccination with monovalent inactivated hepatitis A vaccines—a systematic review. Hum Vaccin Immunother. https://doi.org/10.1080/21645515.2016.1242539
27. Hegde NR, Gore MM (2017) Japanese encephalitis vaccines: immunogenicity, protective efficacy, effectiveness, and impact on the burden of disease. Hum Vaccin Immunother. https://doi.org/10.1080/21645515.2017.1285472
28. Vidor E, Plotkin SA (2013) Poliovirus vaccine—inactivated. Vaccines, 6th edn. Elsevier Saunders, Philadelphia
29. Xing Y, Schmitt HJ, Arguedas A, Yang J (2017) Tick-borne encephalitis in China: a review of epidemiology and vaccines. Vaccine. https://doi.org/10.1016/j.vaccine.2017.01.015
30. Schneweis KE, Gruber J, Hilfenhaus J, Möslein A, Kayser M, Wolff MH (1981) The influence of different modes of immunization on the experimental genital herpes simplex virus infection of mice. Med Microbiol Immunol. https://doi.org/10.1007/BF02125526
31. Cappel R (1976) Comparison of the humoral and cellular immune response after immunization with live, UV inactivated herpes simplex virus and a subunit vaccine and efficacy of these immunizations. Arch Virol. https://doi.org/10.1007/BF01317862
32. Gao Q, Zhao S, Qin T, Yin Y, Yu Q, Yang Q (2016) Effects of inactivated porcine epidemic diarrhea virus on porcine monocyte-derived dendritic cells and intestinal dendritic cells. Res Vet Sci. https://doi.org/10.1016/j.rvsc.2016.03.023
33. Zahorska R, Mazur N, Korbecki M (1978) Immunogenicity of UV-inactivated measles virus. Zentralbl Bakteriol Orig A. 240(4):424-30.

34. Selimov M, Aksenova T, Klyueva E, Gribencha L, Lebedeva I (1978) Evaluation of the inactivated tissue culture rabies vaccine from the Vnukovo-32 strain. Results of its industrial production and field use for post-exposure immunization of man. Dev Biol Stand. 40:57-62.
35. Marthas ML, Miller CJ, Sutjipto S, Higgins J, Torten J, Lohman BL, Unger RE, Ramos RA, Kiyono H, McGhee JR et al (1992) Efficacy of live-attenuated and whole-inactivated simian immunodeficiency virus vaccines against vaginal challenge with virulent SIV. J Med Primatol. 21(2-3):99-107.
36. Bresler S, Kolikov V, Katushkina N, Molodkin V, Friedman E, Zheleznova H, Malafeieva L, Peradze T, Beljakov V, Ivanov K (1975) Immunogenicity of inactivated influenza vaccine, purified by adsorption chromatography on porous glas. Med Biol. 53(6):456-61.
37. Iwata-Yoshikawa N, Uda A, Suzuki T, Tsunetsugu-Yokota Y, Sato Y, Morikawa S, Tashiro M, Sata T, Hasegawa H, Nagata N (2014) Effects of Toll-like receptor stimulation on eosinophilic infiltration in lungs of BALB/c mice immunized with UV-inactivated severe acute respiratory syndrome-related coronavirus vaccine. J Virol. https://doi.org/10.1128/JVI.00983-14
38. Lo CW, Matsuura R, Iimura K et al (2021) UVC disinfects SARS-CoV-2 by induction of viral genome damage without apparent effects on viral morphology and proteins. Sci Rep 11:13804. https://doi.org/10.1038/s41598-021-93231-7
39. Mathew AM, Mun AB, Balakrishnan A (2018) Ultraviolet inactivation of Chikungunya virus. Intervirology. https://doi.org/10.1159/000490567
40. Darnell ME, Subbarao K, Feinstone SM, Taylor DR (2004) Inactivation of the coronavirus that induces severe acute respiratory syndrome, SARS-CoV. J Virol Methods. https://doi.org/10.1016/j.jviromet.2004.06.006
41. List of Classifications—IARC monographs on the identification of carcinogenic hazards to human. https://monographs.iarc.who.int/list-of-classifications. Accessed 23 Feb 2021
42. Heilingloh CS, Aufderhorst UW, Schipper L, Dittmer U, Witzke O, Yang D, Zheng X, Sutter K, Trilling M, Alt M, Steinmann E, Krawczyk A (2020) Susceptibility of SARS-CoV-2 to UV irradiation. Am J Infect Control. https://doi.org/10.1016/j.ajic.2020.07.031
43. Gu H, Chen Q, Yang G et al (2020) Adaptation of SARS-CoV-2 in BALB/c mice for testing vaccine efficacy. Science. https://doi.org/10.1126/science.abc4730
44. Muruato A, Vu MN, Johnson BA, Davis-Gardner ME, Vanderheiden A, Lokugamage K, Schindewolf C, Crocquet-Valdes PA, Langsjoen RM, Plante JA, Plante KS, Weaver SC, Debbink K, Routh AL, Walker D, Suthar MS, Shi PY, Xie X, Menachery VD (2021) Mouse-adapted SARS-CoV-2 protects animals from lethal SARS-CoV challenge. PLoS Biol. https://doi.org/10.1371/journal.pbio.3001284
45. Kant R, Kareinen L, Smura T, Freitag TL, Jha SK, Alitalo K, Meri S, Sironen T, Saksela K, Strandin T, Kipar A, Vapalahti O (2021) Common laboratory mice are susceptible to infection with the SARS-CoV-2 beta variant. Viruses. https://doi.org/10.3390/v13112263
46. National Research Council (US) (2011) Committee for the update of the guide for the care and use of laboratory animals. Guide for the Care and Use of Laboratory Animals. 8th ed. Washington (DC): National Academies Press (US); 2011.